Surface Roughness Observation of Arctic Ice Using Low Grazing Angle Radar

Armin Parsa
R&D Department
Rutter Inc.
St. John's, Canada
Email: aparsa@rutter.ca

***Abstract*— The surface roughness of Arctic ice is observed by calculating the correlation coefficient between the co-polarized and cross-polarized radar returns. The radar data is collected in the eastern Arctic by the Canadian Coast Guard Ship (CCGS) Henry Larsen, which is equipped with an X-band radar capable of measuring co-polarized and cross-polarized radar return signals. The correlation coefficient is calculated locally for each pixel at the center of a two-dimensional template window. To reduce the computational cost, the two-dimensional radar image is divided to smaller sub-windows, and the local correlation coefficient is obtained for each sub-window.**

I. INTRODUCTION

Information about soil surface roughness has been extracted from polarimetric synthetic aperture radar (SAR) data and co-polarized correlation coefficient [1]. It is shown that the surface roughness can be detected by calculating the coherence between different polarization components [2]. Polarimetric SAR has also been used to classify the ice type and ice thickness based on the ice depolarization factor [3-4]. Although satellite data can provide useful information for characterizing the ice type, satellite services are relatively expensive for providing high resolution imagery. Furthermore, there are not many satellites that can pass close enough to the high Arctic regions for their sensors to collect data there, and they are limited by coverage time. It is very useful for vessels to have an on-board X-band radar for real-time ice navigation. For this type of radar, the sea ice is illuminated at near-grazing incidence angles, and the radar return is prone to multipath interference.

The CCGS Henry Larsen undertook a large data collection program to record, and collect radar data of Arctic sea ice during several weeks in August 2012. The CCGS Henry Larsen has an on-board X-band radar that can measure the co-polarized and depolarized radar return.

This paper presents the results obtained by calculating the local correlation coefficient between the co-polarized and cross-polarized return signal to observe the ice surface roughness. The effect of window size and scan-to-scan integration is observed when displaying the ice surface. To improve the computational time, the image is divided into sub-images, and all the pixels of each sub-image are filled with the maximum of the normalized cross-correlation which is obtained for each sub-image.

II. DATA ANALYSIS AND RADAR SETTINGS

The correlation coefficient is usually used for comparing the similarity between two images and it is given by

$$\rho_{HHHV} = \frac{\sum_{i,j}(x_{ij} - x_m)(y_{ij} - y_m)}{\sqrt{\sum_{i,j}(x_{ij} - x_m)^2}\sqrt{\sum_{i,j}(y_{ij} - y_m)^2}} \quad (1)$$

where x_{ij} and y_{ij} represent the pixel intensity of the first and second images (in the i^{th} row and j^{th} column), respectively. Furthermore, x_m and y_m are the mean intensity of first and second images, respectively.

The two images that will be compared here are the co-polarized and cross-polarized radar images. Due to bistatic configuration of the radar antennas, the range and/or azimuth offset between co-polarized (HH) and cross-polarized (HV) sub-images must be considered. As a result, the correlation coefficient is obtained by calculating the peak of the cross-correlation matrix. The elements of the cross correlation matrix are obtained as

$$\rho_{HHHV}(k,n) = \frac{\sum_{i,j}(x_{ij} - x_m)(y_{(i+k)(j+n)} - y_m)}{\sqrt{\sum_{i,j}(x_{ij} - x_m)^2}\sqrt{\sum_{i,j}(y_{(i+k)(j+n)} - y_m)^2}}. \quad (2)$$

The data recording was performed in the month of August 2012. This paper uses data recorded at Hall Basin (shown in Fig. 1) on August 7th, 2012. A satellite image of the region captured by NASA Aqua satellite is available at [5] and is shown in Fig. 2. The ice chart provided by Canadian Ice Service is shown in Fig. 3, and shows the type of sea ice

2013 IEEE Radar Conference (RadarCon13)
978-1-4673-5794-4/13/$31.00 ©2013 IEEE

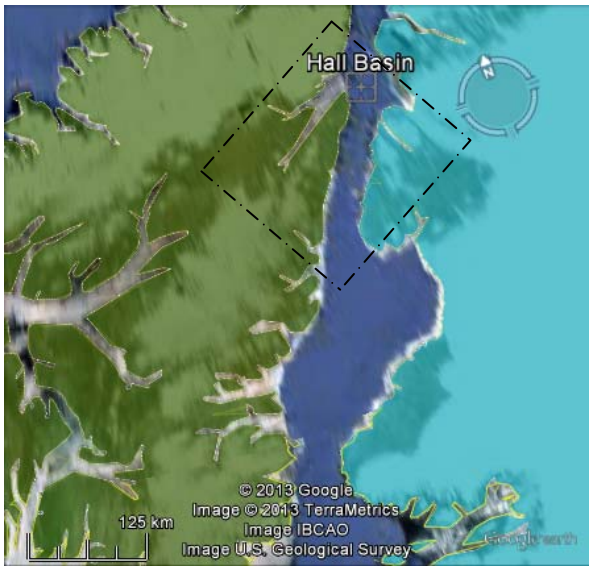

Figure 1: Location of the CCGS Henry Larsen on the map at Hall Basin during the trial.

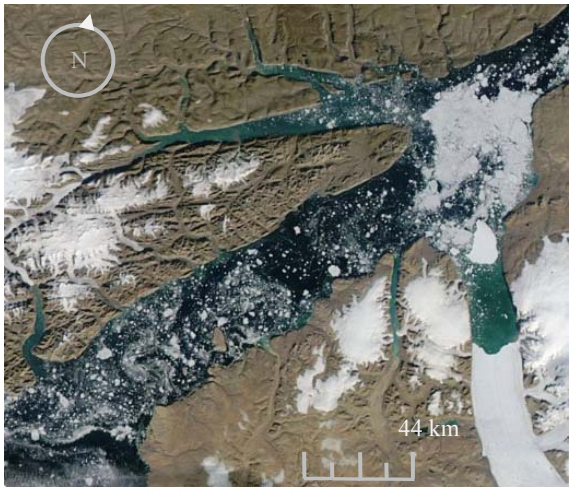

Figure 2: NASA Satellite image of Hall Basin [5] taken on Aug. 06, 2012. The location of this image is shown in Fig. 1 and Fig. 3 by a dash-dotted rectangle.

present during the data collection on August 7th, characterized as old, multi-year ice. Two radar antennas and two transceivers were used during the trial, with the horizontal polarized antenna transmitting and receiving (HH) and the vertical polarized antenna receiving (HV) simultaneously. The rotations of the two antennas were synchronized so that the main beams of the two antennas were always pointing in the same direction with a bistatic configuration. The spacing between the two antennas was 4 m. The radar specifications of the HH and HV antennas and transceivers are given in Table I.

TABLE I. THE RADAR SYSTEM SPECIFICATION OF HH AND HV ANTENNAS AND TRANSCIEVERS

	HV	HH
Antenna Gain (dB)	28	31
Antenna Polarization	Vertical	Horizontal
Antenna Beamwidth (degree)	2	0.9
Transmitter Peak Power (KW)	25	25
Operating Frequency (GHz)	9.41	9.41
Pulse Length (ns) [Short/Medium/Long]	50/250/750	50/250/750
IF Bandwidth (MHz)	20	20
Overall Noise Figure (dB) ≤	5	5
Side Lobes (dB) ≤	-30	-30
PRF (Hz) [Short/Medium/Long]	3000/1800/785	3000/1800/785
Antenna Rotation Speed (rpm)	30/45/60/120	30/45/60/120

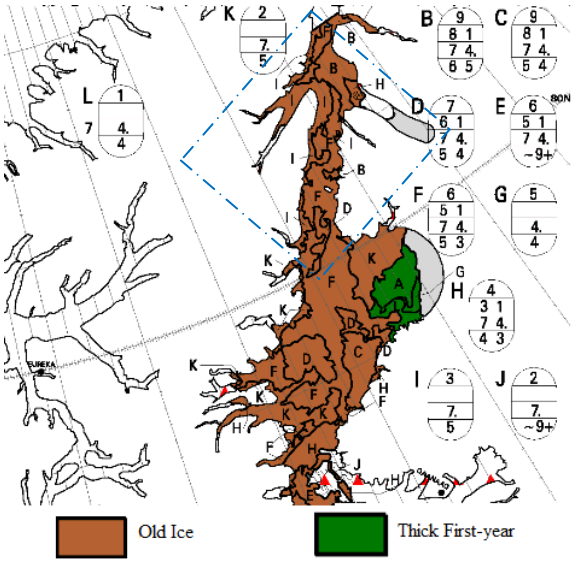

Figure 3: Canadian ice chart[1] [6] on August 7th, 2012 has characterized the sea ice at Hall Basin as old ice (has survived at least one summer).

I. RESULTS

In order to have close to real time analysis, it has been performed on a segment of the B-scan images recorded by HH and HV receivers, using Rutter's *sigma* S6 system [7]. Fig. 4(a) and Fig. 4(b) display the recorded HH and HV B-scan images, respectively. The image contains a large old ice floe depicted between 0.2 and 0.4 nmi with a triangular shape and a highly illuminated front edge. The radar heading was at 295.4 degrees. Each pixel occupies 3.75 m along range axis and 0.2344 degrees along the azimuth direction. Since the short pulse was used for this recorded data, the radar range resolution is 7.5 m for both channels. The antenna with vertical polarization has an antenna beamwidth of 2 degrees, while the beamwidth of the antenna with the horizontal polarization is 0.9 degrees. Since the antenna with vertical polarization is in receive mode, the 0.9 degree illumination by the horizontally polarized antenna defines the azimuth resolution of the HV channel.

Fig. 5 shows the local correlation coefficient obtained for each pixel of the image. A rectangular template window is

[1]The reproduction is a copy of an official work that is published by the Government of Canada and the reproduction has not been produced in affiliation with or with the endorsement of the Government of Canada.

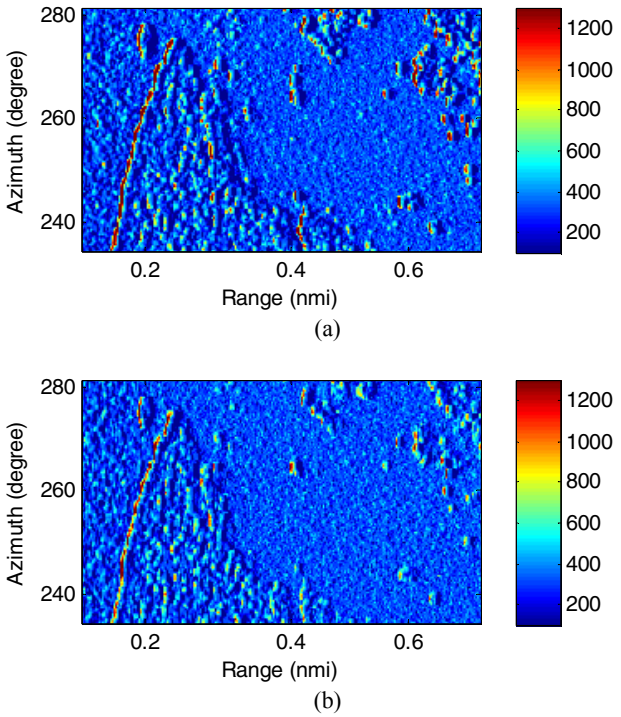

Figure 4: Part of a B-scan radar image which contains a multiyear ice floe recorded using a) HH, and b) HV polarization.

used for calculating the local correlation coefficient at the center of the window. The effect of window size w is observed on the calculated results. For all cases, the edge of the ice floe gives a very high correlation coefficient value. The ice edge observed by correlation coefficient becomes wider when the window size is increased. The correlation coefficient is higher for the sea water surface at closer range due to clutter which contributes to surface roughness. The surface roughness is more detectable since the angle of incidence becomes larger (the angle of incidence is measured from the sea surface). Assuming that the surface roughness is directly proportional to the correlation coefficient value, it is observed that the roughness of the ice floe is higher than the sea water at close range (sea water at range <0.2 nmi). As well, some ice areas show higher correlation coefficient values, indicating rougher surface with sharp edges, capable of depolarizing horizontally polarized microwaves.

For real time scenarios, calculating the local correlation coefficient requires expensive computer resources, and the computational cost becomes higher when the window size increases. As a result, the local correlation coefficient calculation is not suitable for real time analysis. A faster approach is to divide the image into rectangular sub-images and calculate the cross-polarization for each sub-image as shown in Fig. 6. When the sub-image size is 20×20 pixels (referring to Fig. 6(c)), the ice surface can be differentiated from the sea surface at close range since the ice surface shows higher roughness than the sea surface at close range. The CPU time needed for calculating the results shown in Fig. 5 and Fig. 6 are given in Table II.

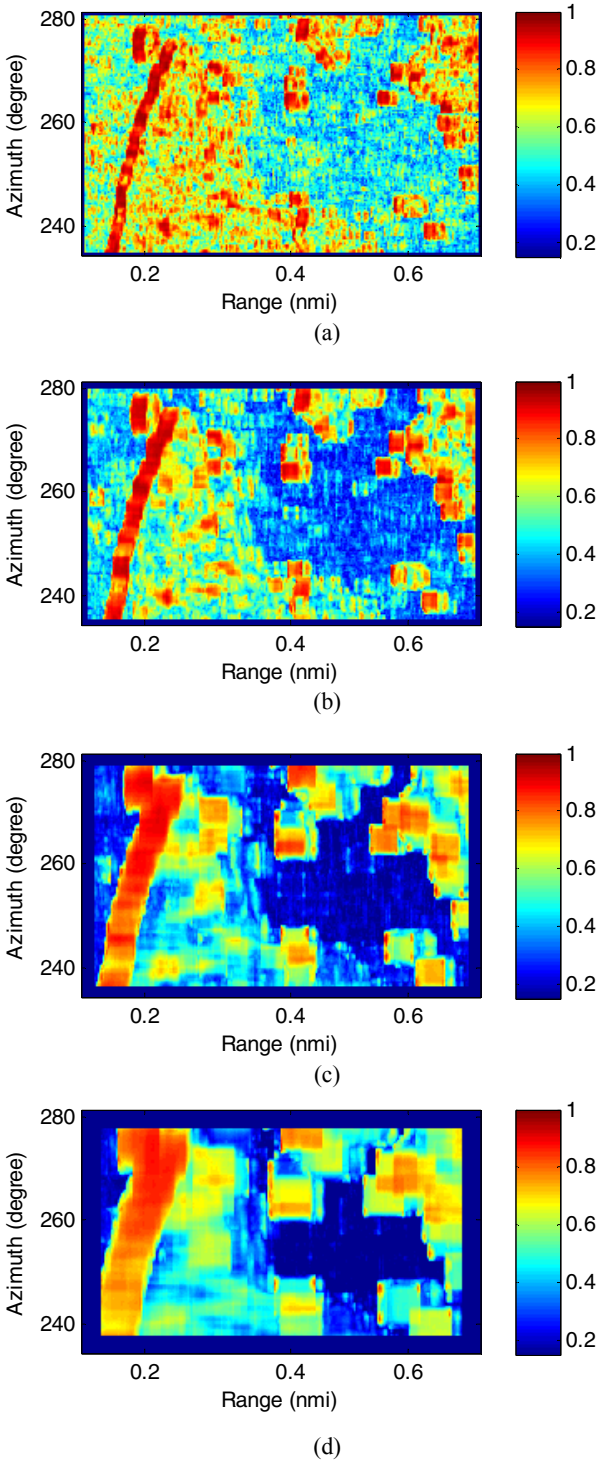

Figure 5: Local correlation coefficient between HH and HV image using a $w \times w$ pixel window when a) w =7, b) w =11, c) w =21, and d) w =31 pixels. Each pixel occupies 3.75 m along range axis and 0.2344 degrees along the azimuth direction.

Fig. 7(a) and Fig. 7(b) show the HH and HV channels when scan-to-scan integration is applied with 10 scans averaged and integrated. Comparing Fig. 7(c) with Fig. 5(b)

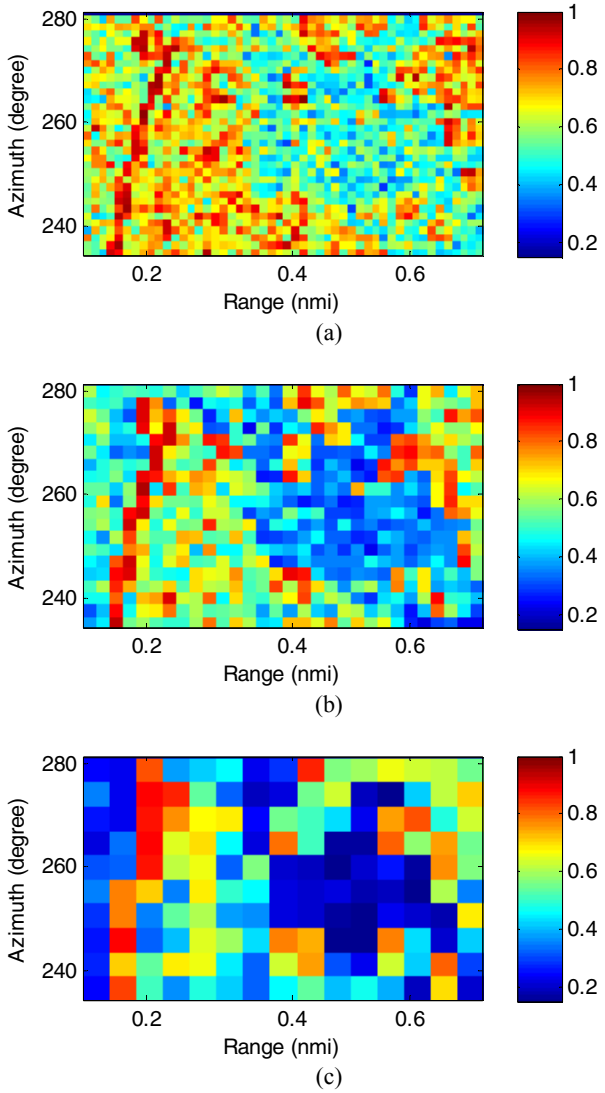

Figure 6: Local correlation coefficient of sub-images when the image is divided into sub-images. All pixels of each sub-image are filled with the correlation coefficient obtained for each sub-image. Sub-image sizes are a) 6×6, b) 10×10, and c) 20×20 pixels.

and Fig. 7(d) with 6(a), it is easier to differentiate the surface of the ice floe from sea clutter by the correlation coefficient obtained from scan averaged images.

Fig. 8 (a) and Fig. 8 (b) show a part of scan converted radar image (intensity levels) recorded with HH and HV polarizations at 21:04:39 UTC on August 7th, 2012, respectively. The images of local correlation coefficients using a sliding window with a size $w = 7$ and $w = 21$ pixels are

TABLE II. CPU TIME REQUIRED FOR CALCULATING THE RESULTS SHOWN IN FIG. 5 AND FIG. 6.

	Sliding Windows				Sub-image Windows		
Window Size (pixels)	7	11	21	31	6	10	20
CPU Time (seconds)	4.6	5.6	21.5	61.8	0.2	0.11	0.07

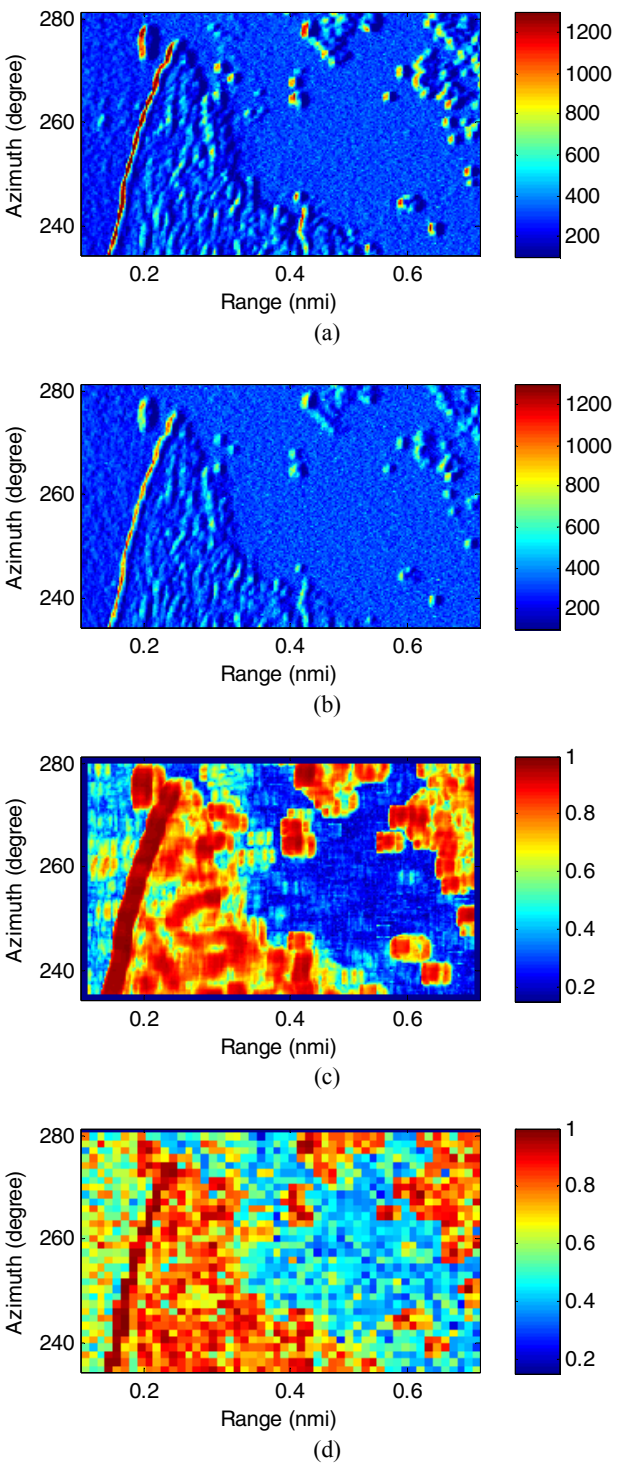

Figure 7: B-scan radar image containing a multiyear ice floe after integrating 10 scans (10 scans are averaged) with a) HH, b) HV polarization. c) Local correlation coefficient for the HH and HV images after applying scan-to-scan integration. The local correlation coefficient is obtained at the center of a sliding 11×11 pixel window. d) Local cross-correlation of HH and HV images is calculated when the image is divided into 6×6 pixel sub-images. All the pixels of each sub-image are filled with the correlation coefficient obtained for each sub-image.

shown in Fig. 8 (c) and Fig. 8 (d), respectively. Comparing Fig. 8 (c) and Fig. 8 (d), the ice edges show higher correlation

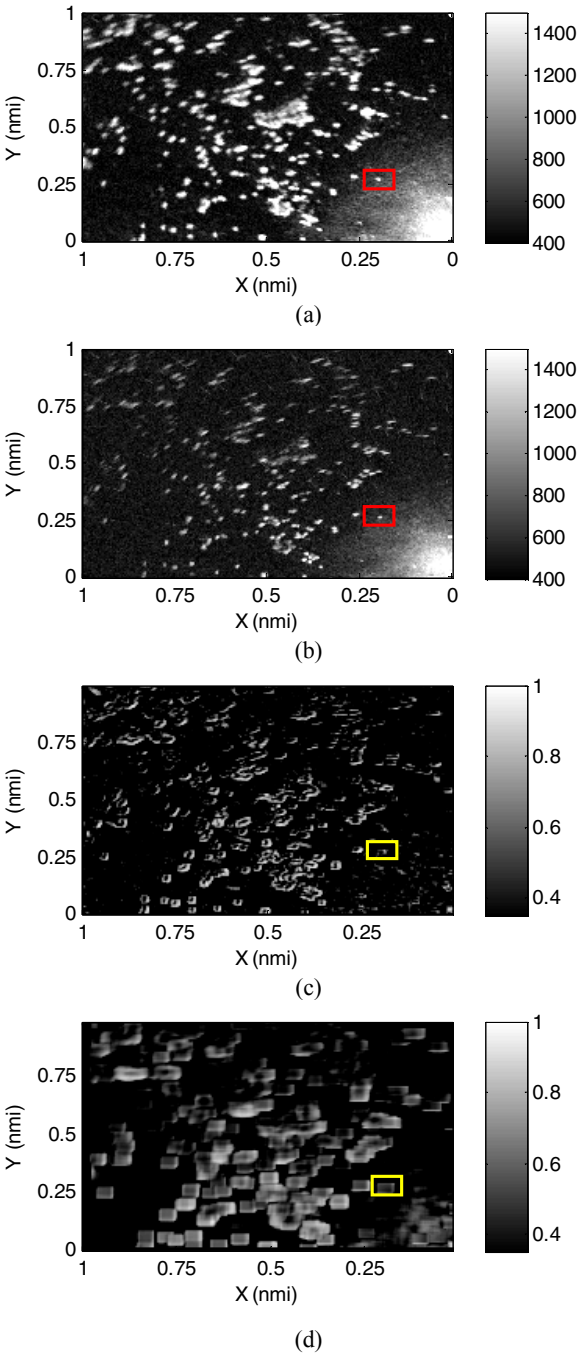

Figure 8: Part of scan converted image with a) HH polarization, and b) HV polarization. The local correlation coefficient between HH and HV image calculated using a sliding window with the size c) w =7 pixels, and d) w =21 pixels. The maximum correlation coefficient inside the yellow rectangle is plotted versus range in Fig. 9 as the CCGS Henry Larsen gets closer to a growler shown inside the red rectangle.

coefficient when smaller window size is used.

Fig. 9 shows the maximum correlation coefficient calculated with a window size w = 7 and w = 21 pixels for a growler [shown inside the red rectangle in Fig. 8 (a)] versus range as the CCGS Henry Larsen moves toward the growler. It is observed that the correlation coefficient is decreased by increasing the window size. Furthermore, the correlation

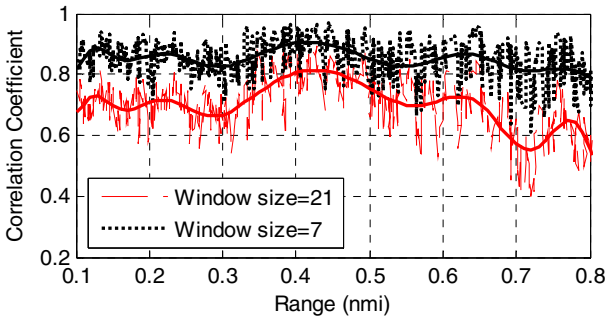

Figure 9: Maximum correlation coefficient obtained for a growler shown inside the red rectangle in Fig. 8(a). Dashed and dotted lines show the actual values versus range, while solid lines show the fitted curves.

coefficient variation as a function of range is observed.

II. Conclusions

The local correlation coefficient is calculated for the co-polarized and cross-polarized return signal to detect the ice surface roughness. First, the local correlation coefficient was obtained for each pixel at the center of a sliding window. The effect of window size was observed for several cases. The computational time was improved by dividing the image into sub-images, and calculating the correlation coefficient for each sub-image. The scan-to-scan integration was applied to both HH and HV channels. The correlation coefficient of the scan-to-scan integrated images showed a better performance in distinguishing the ice roughness from sea water at close range.

It was shown that the correlation coefficient becomes smaller by increasing the window size. Since the only ground-truth data available was the Canadian Ice Charts, it was not possible to calibrate the data in this trial. As a future work, it would be suggested to calibrate the cross-polarized radar system on the CCGS Henry Larsen using the Radarsat 2 cross-polarized satellite imagery.

Acknowledgment

The author wishes to thank the Canadian Coast Guard for providing the recorded data, S Hale, D. Smith, and T. Healy for providing helpful comments and suggestions.

References

[1] F. Mattia, T. L. Toan, J.-C. Souyris, G. De Carolis, N. Floury, F. Posa, G. Pasquariello, "The Effect of surface roughness on multifrequency polarimetric SAR data," IEEE Trans. Geosci. Remote Sensing, vol. 35, pp. 954-966, 1997.

[2] D. Kasilingam, D. Schuler, and J. S. Lee, "The depolarization of radar backscatter from rough surfaces due to surface roughness and slopes," Proc. IGARSS, pp. 925-927, 2001.

[3] J.-W. Kim, D.-J. Kim, B. J. Hwang, "Characterization of arctic sea ice thickness using high-resolution spaceborne polarimetric SAR data," IEEE Trans. Geosci. Remote Sensing, vol. 50, pp. 13–22, Jan 2012.

[4] M. Arkett, D. Flett and R. D. Abreu, "C-band multiple polarization SAR for sea-ice monitoring – what can it do for the Canadian Ice Service," Proceedings of Envisat Symposium, 23-27 April 2007.

[5] Centre for Ocean and Ice-Danish Meteorological Institute, http://ocean.dmi.dk/arctic/modis.uk.php

[6] Canadian Ice Service (CIS), Environment Canada, www.ec.gc.ca

[7] *sigma* S6 Ice Navigator Radar Processor, 2010. [online] Available: http://www.rutter.ca